Journal of Physiology (1993), **465**, *pp.* 245–263
With 8 figures
Printed in Great Britain

QUANTIFICATION OF EXPONENTIAL Na^+ CURRENT ACTIVATION IN *N*-BROMOACETAMIDE-TREATED CARDIAC MYOCYTES OF GUINEA-PIG

BY TAMOTSU MITSUIYE AND AKINORI NOMA

From the Department of Physiology, Faculty of Medicine, Kyushu University, Fukuoka 812, Japan

(*Received 30 March 1992*)

SUMMARY

1. The activation kinetics of the Na^+ current was investigated in single ventricular cells of the guinea-pig heart using an improved oil-gap voltage clamp method. The inactivation of the current was removed by an intracellular application of *N*-bromoacetamide (NBA) for less than 1 min. Although the NBA treatment slightly decreased the peak amplitudes ($81{\cdot}7 \pm 13{\cdot}4$% of control, $n = 15$), the Na^+ current remained stable after the removal of inactivation.

2. On depolarization, the activation of Na^+ current took an exponential time course after the capacitive current decreased to 5% of its peak amplitude (40–100 μs after the pulse onset). The time course of deactivation, recorded on repolarization from 1·2 ms depolarization, was also a single exponential.

3. The time constants of activation and deactivation were almost identical when compared at a given test potential within a range of -50 to -30 mV. These findings indicate that the cardiac Na^+ current activation is determined by m^1 kinetics, or one rate-limiting step.

4. At potentials negative to -60 mV, the deactivation was complete, and its time constant decreased e-fold per $20{\cdot}3 \pm 1{\cdot}8$ mV hyperpolarization ($n = 7$).

5. The degree of steady-state activation ($m(\infty)$) was fitted to a Boltzmann equation with a slope factor of $7{\cdot}4 \pm 0{\cdot}3$ mV and a half-maximum potential of $-33{\cdot}3 \pm 0{\cdot}8$ mV ($n = 8$).

6. Rate constants for the rate-limiting activation step between a closed state and an open state (α_m, β_m), were determined from $m(\infty)$ and τ_m over a potential range between -100 and $+50$ mV. On a logarithmic scale, $\beta_m{}^{-1}$ was a linear function of the membrane potential over the range -100 and -30 mV.

7. Fitting the newly determined activation kinetics to the rising phase of the action potential indicated that the activation kinetics in the present study is relevant to the physiological action potential. The density of the Na^+ channels thus obtained was 1075 ± 186 pF^{-1} ($n = 6$).

8. The measurements in the NBA-treated Na^+ current were compared with those obtained without treatment.

MS 1247

INTRODUCTION

The kinetics of cardiac Na^+ current has been well explained or evaluated in most excitable tissues based on the classical Hodgkin–Huxley-type model (Hodgkin & Huxley, 1952), in which at least three state transitions were assumed for the channel activation. In a previous study of cardiac myocytes, however, Mitsuiye & Noma (1992) reported that the activation time course of cardiac Na^+ current is not sigmoidal, but exponential when recorded with an improved oil-gap voltage clamp technique. The effective series resistance was successfully reduced to less than 40 KΩ, and the maximum amplitude of Na^+ current was limited to less than 30 nA. When compared at a given potential, the time constant of activation closely corresponded to that of deactivation. Thus, a single rate-limiting step was suggested in the activation process. However, the activation kinetics of the Na^+ current were isolated from the inactivation by assuming an h-gate, which was independent from the activation m-gate (Hodgkin & Huxley, 1952). Although this assumption was useful in analysing Na^+ current, it did not allow for a qualitative determination of the activation kinetics. Furthermore, recent single channel studies have suggested that the time course of inactivation of the macroscopic Na^+ current attributes much to activation kinetics (Berman, Camardo, Robinson & Siegelbaum, 1989; Yue, Lawrence & Marban, 1989; Scanley, Hanck, Chay & Fozzard, 1990).

The chemical removal of inactivation using protein-specific reagents enabled the analysis of the Na^+ channel activation in its purified state in the nerve (Oxford, 1981; Stimers, Bezanilla & Taylor, 1985). In this study, we removed inactivation of the Na^+ current by the intracellular perfusion of single myocytes with *N*-bromoacetamide (NBA) taking advantage of the oil-gap method. The reduction of the amplitude of Na^+ current (Oxford, Wu & Narahashi, 1978; Horn, Vandenberg & Lange, 1984; Gonoi & Hille, 1987) was minimized by washing out the NBA quickly after a partial reduction in the inactivation. The adequacy of m^1 kinetics was confirmed and the rate constants for the rate-limiting step between a closed state and an open state were thus determined based on a new activation model. The number of open channels was determined during the rising phase of the action potential by fitting the model to the recorded action potential.

METHODS

Preparations

The heart was dissected from a guinea-pig under deep anaesthesia from pentobarbitone (50 mg kg^{-1}). The method of obtaining single cells from guinea-pig ventricles using collagenase was essentially the same as that described elsewhere (Powell, Terrar & Twist, 1980; Isenberg & Klöckner, 1982).

Oil-gap voltage clamp and data analysis

The details of the voltage clamp method using an oil gap has been described in a previous paper (Mitsuiye & Noma, 1992; see also Mitsuiye & Noma, 1987). In brief, the sealing resistance (R_s) higher than 1 GΩ within the oil gap facilitated the series resistance compensation. The effective series resistance left in the recording system was less than 50 kΩ. Since amplitudes of Na^+ currents were limited to less than 30 nA by reducing the membrane area in the external solution, and by decreasing the external Na^+ concentration, deviation of the membrane potential from the command potential was less than 1·5 mV at the peak of the Na^+ current.

The Na^+ current was defined as a tetrodotoxin (TTX)-sensitive component as far as the recordings were available within the same cell. After recording the control Na^+ currents, the same pulse protocol was repeated in the 40 μM TTX-containing solution for computer subtraction. Records in the TTX solution represent the sum of capacitative (I_{cap}), leak (I_{leak}) and gating currents (I_{gc}). When TTX data were not available in the same cell, the linear subtraction method was adopted. Currents in response to small hyperpolarizing voltage steps (10–20 mV; n = 10–40) from −100 mV were averaged and scaled for subtraction of both I_{cap} and I_{leak}. The holding potential was −100 mV throughout the experiment. The electrical circuit of the home-made amplifier, and data acquisition to the computer were the same as in the previous study (Mitsuiye & Noma, 1992). The experimental records obtained with input resistances larger than 1 GΩ were used for data analysis. The curve fitting to current recordings was made using a least-squares algorithm (pattern search method: Colquhoun, 1971). The data provided are expressed as the means ± S.D. (n = number of observations) wherever possible.

Recording the action potential

The current clamp mode of the tight-seal method (Hamill, Marty, Neher, Sakmann & Sigworth, 1981) was applied to single ventricular cells. The rising phase of the action potential was recorded at the same room temperature as in the voltage clamp experiment. Compositions of external and internal solutions were the same as those of the control solutions used in oil-gap voltage clamp studies except for K^+, which was substituted for equimolar Cs^+. The bath solution contained 5·4 mM K^+ and the pipette solution was filled with the internal solution containing 140 mM K^+. The electrode resistance filled with the internal solution was less than 1·2 MΩ.

Solutions

The compositions of internal and external solutions were the same as those used in the previous study (Table 1 in Mitsuiye & Noma, 1992). The control external solution contained (mM): NaCl, 140; CsCl, 5·4; $MgCl_2$, 0·5; $CaCl_2$, 1·8; glucose, 11; and pH was adjusted to 7·4 with 5 mM Hepes-NaOH. The internal solution contained (mM): CsOH, 105; aspartate, 105; $MgCl_2$, 0·5; NaCl, 10·0; K_2ATP, 5·0; EGTA, 5·0; and the pH was adjusted to 7·2 with 5 mM Hepes-CsOH. When the amplitude of Na^+ current was larger than 25 nA in the control solution, the Na^+ concentrations of both the external and internal solutions were reduced by mixing the control external or internal solution with corresponding Na^+-free solutions, so that the Na^+ reversal potential was kept constant. Na^+ was replaced with $Tris^+$ in the Na^+-free external solution, and with Cs^+ in the Na^+-free internal solution. Unless otherwise described, control internal and external solutions were used. TTX (40 μM; Sankyo, Japan) was added to the external solution when necessary. To remove inactivation of Na^+ current, 300–500 μM NBA (Sigma, St Louis, MO, USA) was added to the internal solutions with a readjustment of pH. The NBA solution was freshly prepared before use. All experiments were carried out at room temperature (19 ± 1 °C).

Internal perfusion of cardiac myocytes

Because the effects of NBA were progressive, a quick and complete removal of NBA from the intracellular medium was critical in order to obtain a stable Na^+ current. Figure 1 shows a schematic illustration of the improved oil-gap set-up, and representative results of testing efficiency of intracellular perfusion of different Na^+ concentrations ($[Na^+]_i$). Two inlet tubings were inserted until near the tip of the glass capillary of the internal compartment. Both tubings were connected to reservoirs containing internal solutions of 10 and 140 mM Na^+, respectively, and a constant hydrostatic pressure of 10–20 cmH_2O was applied to the perfusates. Switching the perfusate was performed by closing one of the two tubings by a tiny clip. The external pipette was also perfused continuously with a 140 mM Na^+-Tyrode solution. When an exchange of the external solution was required, two tubings were also introduced to the pipette of the external solution.

Figure 1*A* and *B* shows changes in the peak amplitudes of Na^+ current induced by switching the internal solution. The corresponding original current records are superimposed on the same vertical scale as in the graph. In *A*, the amplitude of Na^+ current recorded at +20 mV was gradually decreased and reversed to an outward current within 15 s after switching $[Na^+]_i$ from 10 to 140 mM. Figure 1*B* shows the recovery time course of the Na^+ current as the 140 mM internal solution was switched back to the 10 mM Na^+ internal solution. Although the initial part of the current overlapped with capacitive current, it is obvious that the peak time of both the inward and outward Na^+ currents remained almost constant, and the inactivation time course did not change

during these processes. It should be noted that these findings are expected only when R_s compensation is adequately done to clamp the actual membrane potential at the same command level. Essentially the same quick exchange of the internal solution (< 30 s) as in Fig. 1 was obtained in the four experiments which examined the efficiency of the internal perfusion.

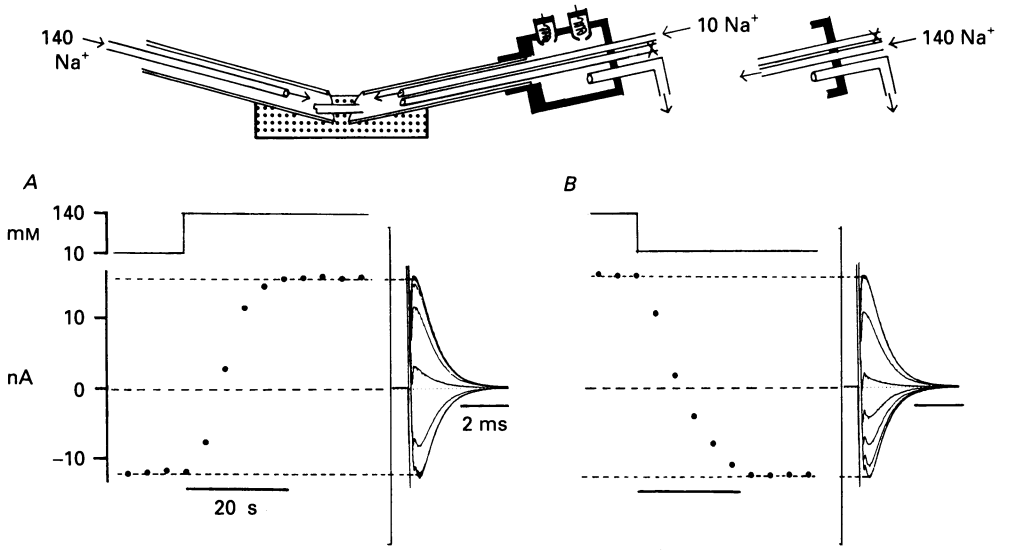

Fig. 1. Schematic illustrations of the improved oil-gap set-up for single cardiac myocytes (above) and experimental records of the Na^+ current on switching $[Na^+]_i$ from 10 to 140 mM (*A*, below) and the recovery (*B*). The internal compartment (right side) was composed of an electrode holder equipped with two agar bridges for voltage sensing and current feeding, respectively, and a glass capillary. Two inlet polyethylene tubes were introduced into the pipette, and the solutions were drained through an outlet tube. In the experiment shown in the lower part, one of the inlet tubings was connected to a reservoir filled with an internal solution of 10 mM $[Na^+]_i$ and the other with 140 mM $[Na^+]_i$ internal solution, and these inlet tubings were clipped alternatively. The single ventricular cell was stretched between the internal (right) and the external compartment (left) in the oil bath (dotted). The external compartment was connected to earth. Lower part: $[Na^+]_i$ is indicated at the top, and the corresponding changes in the peak amplitude of Na^+ current are plotted against the experimental time. The Na^+ current was activated by depolarizing the membrane from −100 to +20 mV every 4 s. The original Na^+ currents are superimposed on the same vertical scale as in the graph (right-hand portions of *A* and *B*). Note the similar time course of individual Na^+ currents having different amplitudes and directions.

RESULTS

Removal of the Na^+ current inactivation

The removal of Na^+ inactivation using NBA was accompanied by a decrease in the current amplitude as described previously in different preparations (Oxford *et al.* 1978; Horn *et al.* 1984; Gonoi & Hille, 1987). The decrease was progressive as long as the application of NBA was continued. To minimize this additional effect, we continuously monitored the Na^+ current after starting the intracellular NBA perfusion in order to switch the perfusate back to the control as soon as an initial sign of modifying Na^+ inactivation was observed. Thereby, the internal perfusion of 300–500 μM NBA was limited to within 1 min using the oil-gap perfusion method.

Figure 2 shows a typical example of removing Na^+ inactivation, where the inactivation during the pulse was progressively slowed down by the NBA treatment. The incomplete inactivation during the pulse resulted in the inward Na^+ tail current on terminating the depolarizing pulse. The peak time of the Na^+ current was slightly

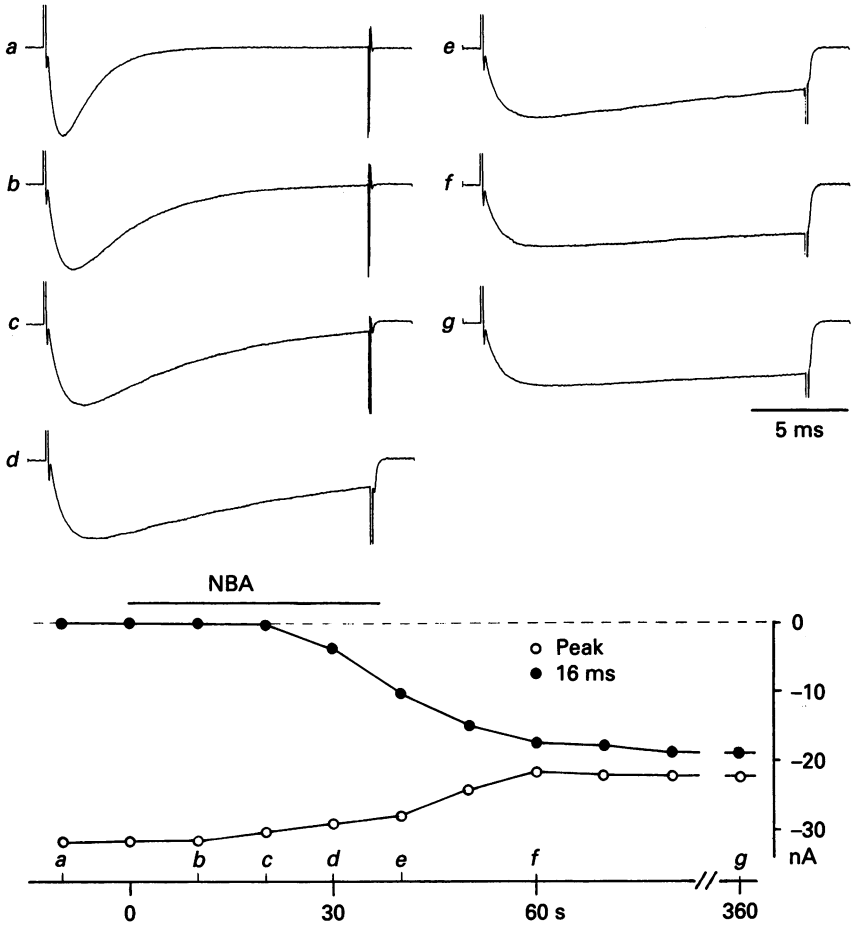

Fig. 2. Effects of internal application of NBA on the Na^+ current, which was recorded every 10 s by a depolarizing pulse to −10 mV from a holding potential of −100 mV. The duration of applying NBA (500 μM) in the internal compartment is indicated above the graph. The upper part shows original recordings (*a–g*) obtained at the experimental times of corresponding characters in the lower graph. The current amplitudes were measured at the peak (○) and at 16 ms after the pulse onset (●).

delayed as the inactivation was removed. Amplitudes of the Na^+ current were measured both at the peak (○) and at 16 ms into the pulse (●), and were plotted against the experimental time in the graph of Fig. 2. The gradual increase of the current amplitude measured at 16 ms indicates the removal of inactivation accompanied by the decrease in the peak Na^+ current amplitude. In this experiment, switching back the perfusate from the NBA solution to the control at 37 s provided a stable Na^+ current having a peak amplitude of 71 % of the control.

After terminating the development of the NBA effect, the modified Na^+ current remained stable throughout the experiment. Only those cells which showed a peak amplitude of more than 50% of control were used for the analysis. In the average of fifteen cells used, the peak amplitude of the Na^+ current at -10 mV was $81{\cdot}4 \pm 13{\cdot}7$%

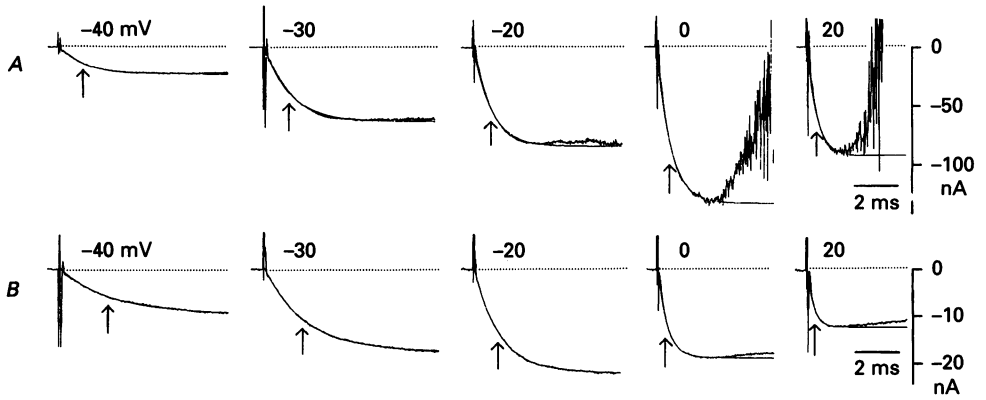

Fig. 3. Comparison of the activation time courses before and after the NBA treatment in the same cell. In *A*, the inactivation was corrected for by extrapolating the exponential curve, which was fitted to the late inactivation phase based on the Hodgkin–Huxley type equations ($I_{Na} = \bar{I}_{Na} m(t)\, h(t)$, I'_{Na} in Mitsuiye & Noma, 1992). In *B*, the inactivation was removed by the NBA treatment. Test potentials are shown. The exponential curves start at time 0 (60 μs after the pulse onset in this experiment). Arrows indicate the time constants of the fitted curves.

of control after the NBA treatment. Exceptionally, two of these cells showed a slight increase (7 and 12%) of the peak amplitude after the NBA treatment.

Activation time course of the NBA-treated Na^+ current

When the time zero for current fitting was set at the time when the capacitive current decayed to 5% of its peak amplitude (Mitsuiye & Noma, 1992), the activation phase was well fitted with a single exponential curve in all records after the NBA treatment (Fig. 3*B*). This single exponential time course was not a result of the NBA treatment. In the experiment shown in Fig. 3, the activation time course was analysed in both the control and the NBA-treated Na^+ currents in the same cell. In the control (*A*), the inactivation time course was first fitted with a sum of two exponentials and the current record was corrected for this inactivation time course based on the Hodgkin–Huxley equations (see I'_{Na} in Mitsuiye & Noma, 1992). At every potential, both the rising phase of I'_{Na} (*A*) and that of the Na^+ current recorded after the NBA treatment (*B*) were well fitted with a single exponential as was the original current. Although the value of the exponential time constant (indicated by the arrow) is clearly larger in the NBA-treated current at potentials negative to 0 mV, this finding rules out the possibility that the NBA treatment modified a sigmoidal Na^+ activation to the exponential time course.

Activation and deactivation at a given membrane potential

Although the activation time course of Na^+ current recorded after the NBA treatment was satisfactory fitted by exponential functions in Fig. 3*B*, slight and

irregular deviations were observed at the very beginning of the current. This was due to a failure in subtracting the capacitive current. Furthermore, current changes are obscured during the capacitive transient. Experimental evidence for the one rate-limiting step, free from these minor difficulties, was obtained by comparing the time constants of activation and deactivation at a given membrane potential.

In Fig. 4, the Na^+ activations on depolarization to -51, -41 and -31 mV were compared with the time course of tail currents at comparable potentials. The tail currents were induced by repolarization from a 1·2 ms depolarizing pulse of -10 mV. All currents were obtained as a TTX (40 μM)-sensitive current in a 140 mM Na^+-Tyrode solution. The amplitude of the Na^+ current near the end of the test pulse of 18 ms was almost equal in each pair of recordings, and a common steady-state level was assumed in fitting theoretical curves. For both currents, fitting of single exponentials was almost perfect, and the time constants of activation and deactivation were similar at a given membrane potential. Essentially similar results were obtained in six other experiments and all the data are listed in Table 1. Thus, both activation and deactivation of the original Na^+ currents recorded after NBA treatment can be described by m^1 kinetics using the same values for $m(\infty)$ and τ_m:

$$I_{Na}(t) = \bar{g}_{Na}(V-E_{Na})\{m(\infty)-(m(\infty)-m(0))\exp(-t/\tau_m)\}. \quad (1)$$

Although the measurements in Table 1 support the m^1 kinetics, the time constants measured from activation seem to be slightly greater than deactivation at -50 mV but not at -30 mV. The ratios of the time constant of activation to that of deactivation at -50, -40 and -30 mV were $1{\cdot}20\pm0{\cdot}04$ ($n=3$), $1{\cdot}07\pm0{\cdot}05$ ($n=7$) and $0{\cdot}80\pm0{\cdot}10$ ($n=5$), respectively. At present we cannot decide whether this is within an experimental error of measurements or due to unknown mechanisms.

TABLE 1. Time constants (ms) of activation and deactivation

	V_t (mV)	Activation	Deactivation		V_t (mV)	Activation	Deactivation
Cell 1	−50	2·05	1·76	Cell 5	−51	2·11	1·72
	−40	2·33	2·24		−41	2·31	2·27
	−30	1·80	2·36	Cell 6	−46	2·29	2·01
Cell 2	−51	1·89	1·58		−41	2·44	2·43
	−41	2·41	2·17		−31	1·97	2·29
	−31	1·90	2·61	Cell 7	−50	2·04	1·89
Cell 3	−40	2·32	2·16		−46	2·10	1·94
	−30	1·81	2·41		−40	2·45	2·31
Cell 4	−46	2·23	1·86		−30	1·95	2·38
	−41	2·26	1·94				
	−35	1·86	2·12				

Voltage dependence of time constants for activation and deactivation of Na^+ current

The exponential time constants measured by fitting the activation time course are plotted over the potential range from -50 to $+50$ mV in Fig. 5 (○). The data points at more negative potentials were obtained from the tail current (●). Representative records of Na^+ tail currents on repolarization to -71, -81, -91 and -100 mV are

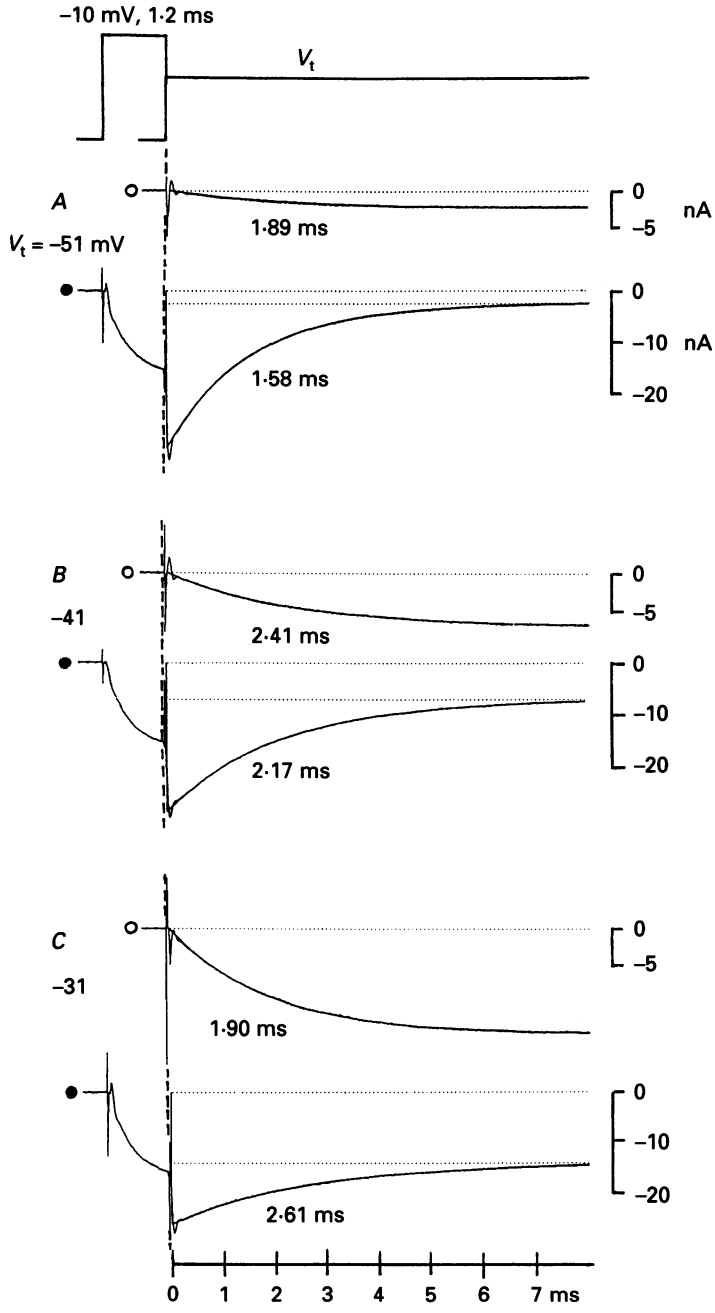

Fig. 4. Comparison of activation and deactivation of the TTX-sensitive Na^+ current at a given membrane potential. The pulse protocol is shown at the top, where the holding potential is -100 mV and the test pulse (V_t) is indicated at the left of each pair of recordings. The currents obtained with single pulse protocol are marked with open circles, while the filled circles indicate the results of the double pulse protocol. Vertical dashed lines indicate the pulse onset, and the dotted lines indicate the current zero level and the window current level. The superimposed single exponential curves start at time 0 (70 μs

shown in Fig. 5*A*, superimposed with single exponential curves. The time constant–voltage relation showed a peak value at −30 to −40 mV and the time constant declined on both sides of the peak, which is expected for a system having one rate-limiting step.

At potentials negative to −55 mV, the degree of activation was negligibly small in the NBA-treated Na^+ current in agreement with the study on the control current (Mitsuiye & Noma, 1992). The tail current levelled off to a zero current level in contrast to the experiment shown in Fig. 4, where the test potentials were less negative. Therefore, the asymptotic line fitted to the voltage relation of time constant of deactivation might simply reflect the voltage dependence of the rate constant of deactivation. In seven experiments, the average of the slope was an e-fold change per 20·3±1·8 mV, which was similar to the values obtained from the normal Na^+ tail currents (21·6±1·3 mV, Mitsuiye & Noma, 1992).

Voltage dependence of the steady-state Na^+ activation

For a complete description of the Na^+ current activation, steady-state activation ($m(\infty)$) was measured as shown in Fig. 6. In this experiment, Na^+ current was obtained as a TTX-sensitive current. The peak amplitude–voltage relation was measured from a family of Na^+ currents, and the limited conductance ($\bar{g}_{Na}$) was approximated by the regression line over the positive slope region. In *B*, steady-state activation (●) was obtained simply by dividing the peak amplitudes by the extrapolated values of the regression line in *A*. The curve superimposed on $m(\infty)$–V plots is the fit of the Boltzmann equation,

$$m(\infty) = \{1+\exp\{(V-V_{half})/s\}\}^{-1}, \quad (2)$$

where $s = 7{\cdot}5$ mV and $V_{half} = -33{\cdot}6$ mV. The averages of s and V_{half} in eight experiments in NBA-treated cells were −33·3±0·8 mV and 7·4±0·4 mV, respectively. Although the value of s was similar to the previous study ($s = 7{\cdot}9\pm0{\cdot}4$ mV, Mitsuiye & Noma, 1992), V_{half} was about 10 mV more negative in the NBA-treated cells ($V_{half} = -21{\cdot}9\pm1{\cdot}7$ mV).

The above analysis of $m(\infty)$ is correct only when $\bar{g}_{Na}$ is constant over the potential range of the measurement of $m(\infty)$. This assumption was justified by confirming the linear 'instantaneous' I–V relationship over the potential range of the $m(\infty)$ curve as demonstrated in the previous study.

Determination of the rate constants for the m^1 activation kinetics

According to the above findings, one rate-limiting step was assumed for the activation of cardiac Na^+ channel:

$$C \underset{\beta_m}{\overset{\alpha_m}{\rightleftharpoons}} O$$

Scheme 1

after the onset of the pulse in this experiment). Time constants of each exponential are indicated. Note the enlarged scales for the activation current compared with the tail currents.

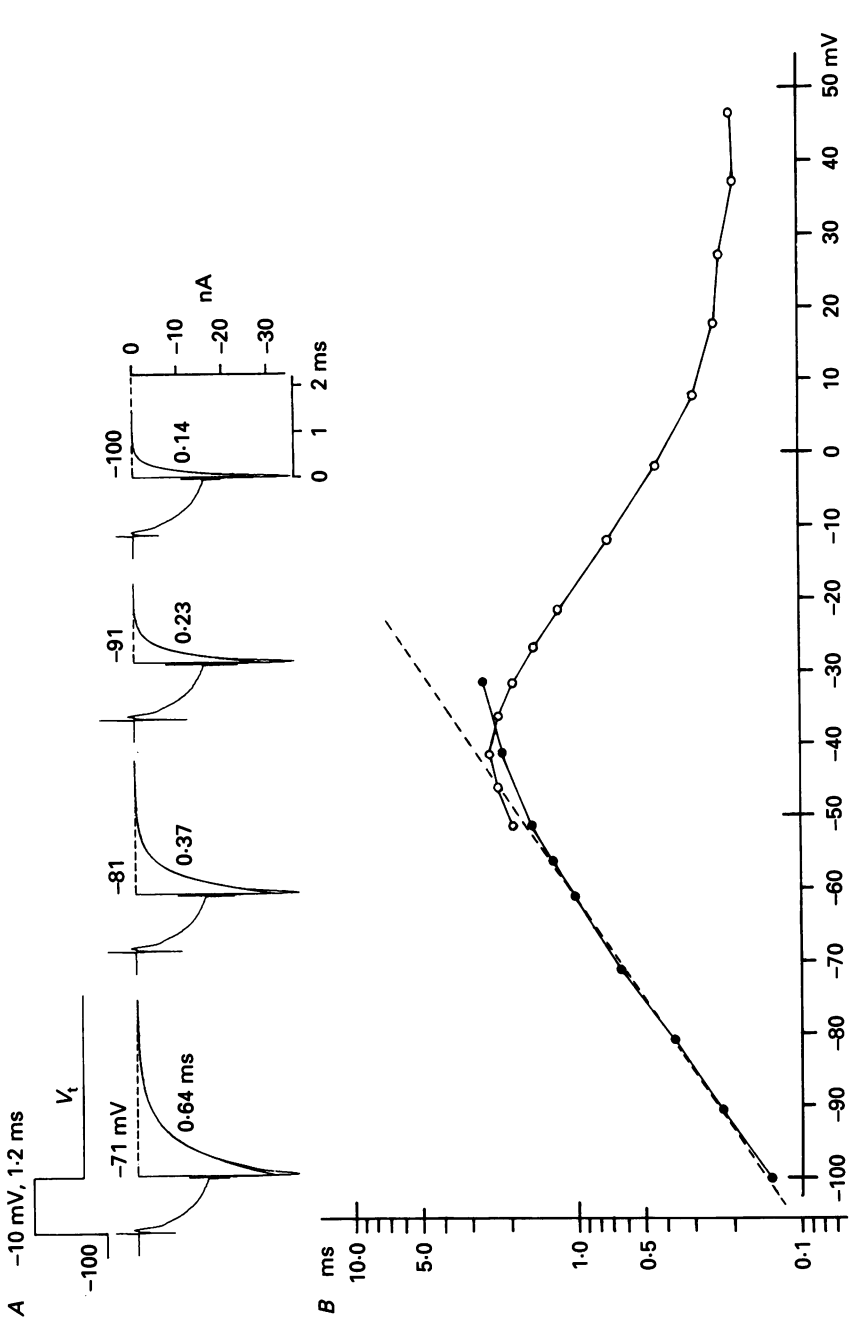

Fig. 5. The relationship between the membrane potential and the time constant for activation kinetics. The fittings of the exponential curve to the tail currents are shown at the top (*A*). The test pulses (V_t) to various levels were applied after a conditioning depolarization to −10 mV for 1·2 ms. The horizontal dashed lines indicate the zero current level, and the exponential time constants are indicated. The time constants thus obtained from the tail current are plotted on a logarithmic scale by the filled circles in the lower graph (*B*). The open circles indicate the exponential time constant obtained by fitting the activation time course of the Na^+ current in the same experiment.

where C is the closed and O the open state. The rate constants for this m^1 activation kinetics were determined from τ_m in Fig. 5 and $m(\infty)$ in Fig. 6.

$$\tau_m = 1/(\alpha_m + \beta_m), \tag{3}$$

$$m(\infty) = \alpha_m/(\alpha_m + \beta_m). \tag{4}$$

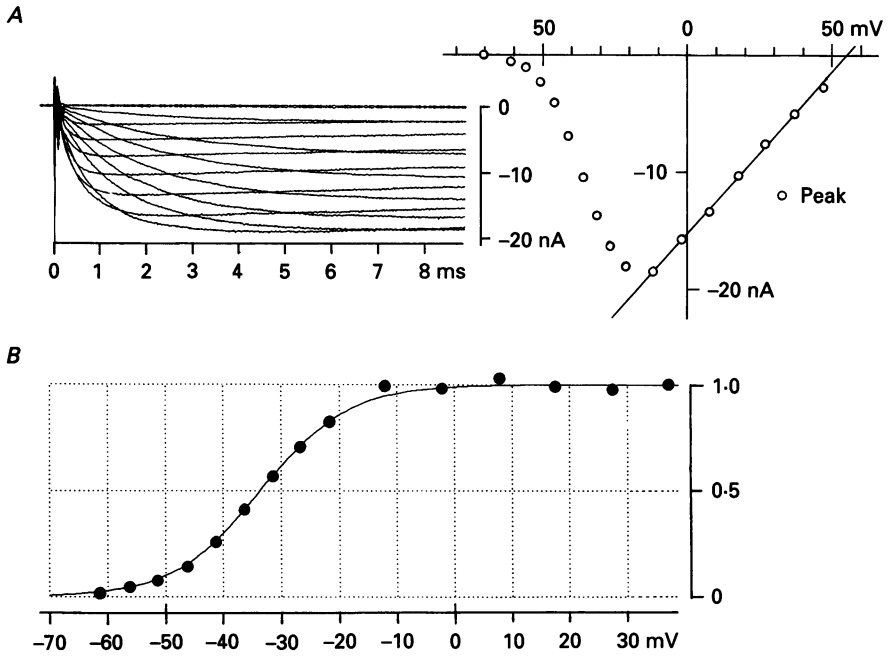

Fig. 6. Steady-state activation of the Na^+ current in the NBA-treated cells. Original current recordings obtained as the TTX-sensitive current are superimposed and their peak amplitudes are plotted on the right. The limited conductance was approximated by a line fitted to the positive limb of the *I–V* curve (*A*). The current amplitudes obtained were divided by the values given by the fitted line at corresponding potentials and results were plotted in the lower graph (*B*).

The reciprocal values of α_m and β_m are plotted on a logarithmic scale against test potentials in Fig. 7*A*. Values of α_m^{-1} and β_m^{-1} obtained from single pulse current (circles), or from tail current (triangles) are in good agreement as shown by common dashed regression lines on the plots. The values of α_m^{-1} deviated from the linear relation positive to −20 mV and seemed to saturate at about 0·2 ms. The maximum slope of the α_m^{-1}–voltage relation was 9·5 mV for an e-fold change in this experiment and was 9·3±0·3 mV for the average of eight experiments. The regression line for β_m^{-1}–voltage relation is the same as that drawn for the τ_m–voltage relation in Fig. 5. The average values of α_m and β_m (s^{-1}) in seven experiments were described as functions of membrane potential, V (mV):

$$\alpha_m(V) = \{102{\cdot}7 \exp(-V/9{\cdot}3) + 250 \exp(-V/150)\}^{-1}, \tag{5}$$

$$\beta_m(V) = \{19832 \exp(V/20{\cdot}3)\}^{-1}. \tag{6}$$

For comparison, the same calculations of α_m and β_m were conducted using the experimental data obtained without using NBA in the previous study (I'_{Na}: Mitsuiye & Noma, 1992). The values of α_m^{-1} and β_m^{-1} were obtained from τ_m and $m(\infty)$ in Figs 6 and 7 in Mitsuiye & Noma (1992), and were plotted in Fig. 7*B*. Values of β_m^{-1}

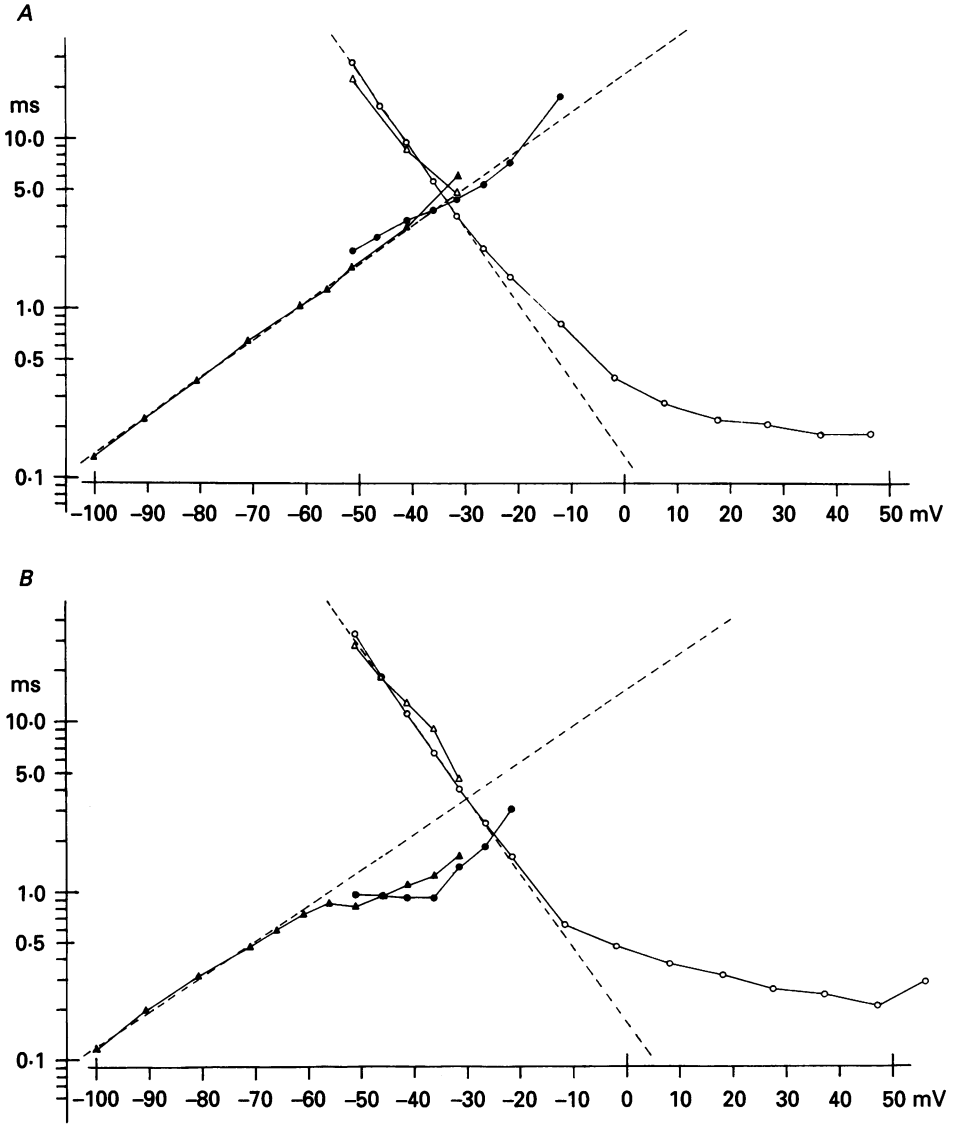

Fig. 7. *A*, rate constants of the activation kinetics obtained from a NBA-treated cell. Open symbols indicate values of α_m^{-1} (circles from the activation time course and triangles from the tail currents), and filled symbols β_m^{-1}. Dashed lines are the visual fit to the plots. Note the larger α_m^{-1} than the values of regression line at more positive potentials. *B*, the same plots as in *A* except that the values were obtained from the Na^+ current corrected for inactivation assuming an independent *h*-gate in Mitsuiye & Noma (1992).

deviated from the linear line fitted to those at potentials negative to −60 mV. This deviation in the β_m^{-1}–voltage relation was different from the present study and may most probably be due to an error in separating the activation kinetics from inactivation by assuming independent *m*- and *h*-gates in the previous study.

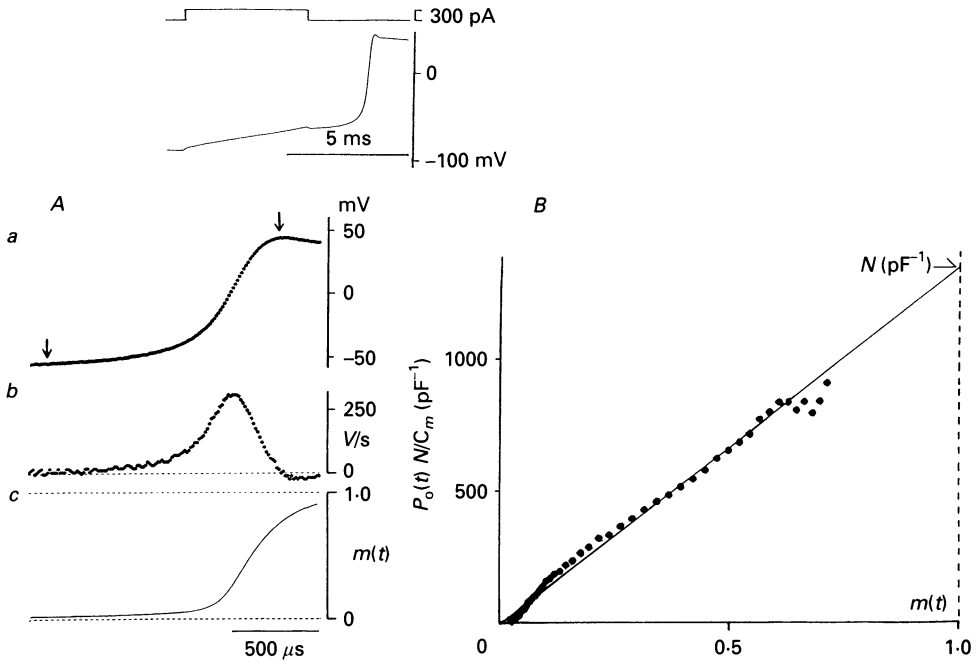

Fig. 8. Activation kinetics during the upstroke of the action potential. *A*, a digitized recording of the rising phase of the action potential (*a*) $dV(t)/dt$ (*b*) and calculated $m(t)$ during the upstroke (*c*). *B*, the relation between $P_o(t)\,N/C_m$ and $m(t)$. Data points between the two arrows (*Aa*) were included. In the inset, the current injection caused a small voltage shift possibly due to a series resistance. To avoid this artificial jump, the amplitude of the current pulse was set to cause the delayed upstroke of the action potential after the cessation of the current pulse. The liquid junction potential between the pipette solution and the Tyrode solution was corrected (10 mV). See text for details.

Estimation of the Na^+ channel activation during the rising phase of the action potential

The relevance of the activation kinetics, newly determined in the present study, was tested by fitting it to the rising phase of the action potential (Fig. 8). Before theoretical treatments of data, experimental results of recording action potentials are summarized as follows. The action potential was elicited by injecting a 5 ms current pulse into the cell under the conventional current clamp mode of the whole-cell patch clamp technique (Hamill *et al.* 1981) as shown in the inset of Fig. 8. In the average of six experiments, the resting potential was $-86{\cdot}1 \pm 0{\cdot}7$ mV and the overshoot was $+44{\cdot}2 \pm 1{\cdot}2$ mV ($n = 6$). The $dV(t)/dt$ was obtained by differentiating the digitized (100 kHz) record of the membrane potential ($V(t)$) (Fig. 8*Ab*). The $\dot{V}_{max}$ was $280{\cdot}6 \pm 24{\cdot}1$ V s^{-1} ($n = 6$) at around 0 mV, which was similar to the value in rat

ventricular cells (230 V s^{-1}: Brown, Lee & Powell, 1981). Smaller values as previously reported in the guinea-pig ventricular cells ($80{\cdot}8 \pm 17{\cdot}7$ V s^{-1} at 25 °C, Hume & Uehara, 1985) were observed only when the resting potential was less negative than -80 mV, and were not used in the present study. The $\dot{V}_{max}$ was not different whether the action potential was initiated immediately or 4 ms after the end of the current injection (not shown), which suggested a very slow development of inactivation at potentials negative to that of the Na^+ current activation. We assume that the development of inactivation is negligible during the rapid upstroke of the action potential.

The m^1 kinetics determined in the present study predicts the time course of m ($m(t)$) during the rising phase of the action potential. The calculation starts from an equilibrium value ($m(\infty)$) at the resting potential, and integrates the following equation for each interval (100 μs) of potential sampling,

$$dm(t)/dt = (1-m(t))\,\alpha_m(V(t)) - m(t)\,\beta_m(V(t)), \tag{7}$$

where $\alpha_m(V(t))$ and $\beta_m(V(t))$ were obtained from eqns (5) and (6) using the mean of two sequential samplings of $V(t)$. The computed values of $m(t)$ were plotted against the experimental time in Fig. 8*Ac*. The value of $m(t)$ at the time of $\dot{V}_{max}$ was $0{\cdot}26 \pm 0{\cdot}03$ ($n = 6$) and continued to increase as the potential reached the overshoot potential.

Independent from the above calculation, the channel open probability ($P_o(t)$) can be derived by dividing the macroscopic current ($I_{Na}(t)$) with the single channel current amplitude ($i_{Na}(t)$):

$$P_o(t) = I_{Na}(t)/(Ni_{Na}(t)), \tag{8}$$

where, N is the total number of channels, and $I_{Na}(t)$ is approximated as,

$$I_{Na}(t) = -C_m\,dV(t)/dt, \tag{9}$$

and

$$i_{Na}(t) = \gamma(V(t) - E_{Na}). \tag{10}$$

Thus, the values of $NP_o(t)/C_m$ during the upstroke of the action potential was experimentally obtained:

$$P_o(t)N/C_m = -dV(t)/dt/\{\gamma(V(t) - E_{Na})\}. \tag{11}$$

γ of 20 pS at 20 °C (Kunze, Lacerda, Wilson & Brown, 1985) and an E_{Na} of +50 mV were used. $NP_o(t)/C_m$ is plotted against $m(t)$ in Fig. 8*B*. It is evident that the experimental measurements of $NP_o(t)/C_m$ is in fact proportional to the theoretical $m(t)$, indicating that the quantification of the m^1 kinetics in the present study is valid. If $P_o(t)$ equals $m(t)$, the linear slope gives a density of distribution of the Na^+ channels (N/C_m), which is 1075 ± 186 pF^{-1} ($n = 6$).

DISCUSSION

m^1 kinetics of Na^+ channel activation

In the present study, inactivation of Na^+ current was removed by a transient intracellular application of NBA, and the activation kinetics were analysed free from

arbitrariness by assuming inactivation mechanisms. The adequacy of m^1 kinetics for Na^+ activation, which was hypothesized in the previous study (Mitsuiye & Noma, 1992), was confirmed in NBA-treated cells, and rate constants for a rate-limiting step between closed and open states were determined.

Our hypothesis for the m^1 kinetics of cardiac Na^+ current activation was not totally different from the experimental findings described in previous studies. Hanck, Sheets & Fozzard (1990) measured the relationship between the membrane potential and the integral of gating charge in single cardiac myocytes using the very fast voltage clamp technique. The potential of half-saturation in the gating charge–voltage relationship was not different from that of the conductance–voltage relation obtained from the peak Na^+ current. This experimental result is different from an expectation from the m^3 kinetics, in which the latter relationship should be observed in a potential range more positive than the former. In the squid giant axon, the $m(\infty)$–voltage relation was comparable to the gating charge–voltage relation, when calculated as a cubic root of the peak Na^+ conductance (see for example, Keynes & Rojas, 1976). Hanck *et al.* (1990) proposed that the first voltage-dependent activation step is rate limiting in the cardiac Na^+ channel.

In the squid axon, the activation time course was successfully analysed based on the m^3 kinetics of a Hodgkin–Huxley type model under the pharmacological removal of inactivation (Oxford, 1981). However, the tail currents on repolarization decayed with a time constant of τ_m instead of one third of τ_m (Fig. 2 in Oxford, 1981). This experimental finding is in line with the view that the rate-limiting step is the last transitional step to channel opening, rather than the m^3 model.

A comparison of the rate constants between the present study and single channel analyses is hampered by the negative shift in the voltage dependence of the gating mechanism in single channel recordings (Cachelin, De Payer, Kokubun & Reuter, 1983; Kunze *et al.* 1985). However, if the shift occurs simply in parallel on the voltage axis (Kimitsuki, Mitsuiye & Noma, 1990), the slope of the relation between rate constants and the membrane potential should be comparable to those in the present study. In a hypothetical Na^+ channel having no inactivation kinetics, α_m^{-1} and β_m^{-1} are equal to the mean latency to the first opening on depolarization and the mean open time, respectively. However, the analysis of the single cardiac Na^+ channels has so far been carried out without the chemical removal of the inactivation gate. Therefore, the mean lifetime cannot solely be attributed to a single rate constant. Yue *et al.* (1989) obtained an equivalent electron charge of $-1{\cdot}3 \pm 0{\cdot}2$ at negative potentials in guinea-pig ventricular myocytes, which corresponds to an e-fold decrease of the mean open time per 19·4 mV hyperpolarization. If the rate constant for inactivation from an open state was negligibly small at negative potentials, the slope may reflect the voltage dependence of β_m. This slope closely agrees with the value of an e-fold decrease of β_m^{-1} per $20{\cdot}3 \pm 1{\cdot}8$ mV obtained in the present study. However, different values have also been reported, most probably depending on a variety of models used for analysis; an e-fold change per 11 mV in canine ventricular cells (Berman *et al.* 1989) using the approach of Aldrich, Corey & Stevens (1983), or an e-fold change per 30 ± 4 mV by fitting data to five states in the Markovian model (Scanley *et al.* 1990).

The rate constant for the last transition to an open state, when measured from the

major component of the first latency histogram, decreased an e-fold per 10 mV between −70 and −40 mV in canine ventricular cells (Berman *et al.* 1989). In canine Purkinje cells, an e-fold change per 30±6 mV was obtained (Scanley *et al.* 1990). The former value may be more straightforward than the latter, and coincides well with an e-fold change of α_m per 9·3±0·3 mV at potentials negative to −20 mV in the present study.

The m^1 kinetics predict a single exponential distribution of the first latency histogram in the single channel analysis in contrast to the peaked distribution in the m^3 kinetics. Experimentally a clear rising phase was described in the first latency histogram of cardiac Na^+ channels and was attributed to the presence of multiple closed states (Grant, Starmer & Strauss, 1983; Kunze *et al.* 1985; Scanley *et al.* 1990). However, the data in the early time after the changing potential have not been quantitatively analysed because of the uncertainty due to the duration of the capacity transient (Grant *et al.* 1983; Scanley *et al.* 1990).

Involvement of the inactivation kinetics in the tail current recorded without using the chemical treatment

In the present study, the peak amplitude of the Na^+ current was decreased by the NBA treatment secondarily to the removal of the inactivation as was the case in various specimens (Oxford *et al.* 1978; Horn *et al.* 1984; Gonoi & Hille, 1987). The decrease of the limited conductance ($\bar{g}_{Na}$) might be attributed to a transition to a new non-conductive state (hibernating state: Horn *et al.* 1984). However, the activation kinetics of the Na^+ channels remaining available after the treatment is not presumed to be largely modified by the NBA treatment. This is because, (1) almost equal asymptotic slopes at negative potentials were obtained in the β_m–voltage relationship before (an e-fold change per 21·6±1·3 mV, Mitsuiye & Noma, 1992) and after (20·3±1·8 mV) the NBA treatment; (2) quantitative measurements of the activation kinetics were very consistent, although the data were collected from different cells, which showed a large variation in the degree of the conductance change after the NBA treatment in the present study.

If one compares the voltage relations of both time constants (Fig. 5) and the steady-state degree of activation (Fig. 6) between the NBA-treated (present study) and the non-treated group (Mitsuiye & Noma, 1992), small differences might be indicated. Unlike the NBA-treated cells, the time constant of activation obtained from normal cardiac cells did not show clear voltage dependence over a potential range of −50 to −20 mV (Fig. 6 in Mitsuiye & Noma, 1992). The voltage relation of steady-state activation in non-treated cells was observed over a potential range about 10 mV more positive than in the NBA-treated cells. These results, when literally interpreted, clearly indicate that NBA changes activation kinetics of Na^+ channels. However, the anomalous non-linear voltage dependence of β_m at potentials of Na^+ activation when calculated from normal Na^+ current (Fig. 7*B*) suggests that these differences can be better explained by the inadequate correction of the inactivation kinetics by assuming an h-gate independent from an m-gate of the Hodgkin–Huxley type.

In the previous study, the time course of the tail current on repolarization was not corrected for the inactivation gate. We assume that the time course of tail current

on repolarization to intermediate potentials is determined by the two steps to the inactivated state (I) and to the deactivated state (C) in the intact cells,

$$C \underset{\beta_m}{\overset{\alpha_m}{\rightleftharpoons}} O \overset{\beta_i}{\rightleftharpoons} I$$

Scheme 2

At potentials near the threshold of Na^+ activation, the magnitude of α_m may be relatively small compared to β_m and the value of β_i might be obtained by subtracting the reciprocal time constant in the NBA-treated cell from that in the non−treated cells. For example, at −50 mV at β_i of 526 s^{-1} is obtained by subtracting the reciprocal time constant in the NBA-treated cell (592 s^{-1}, from Table 1) from that in non-treated cells (1117 s^{-1}, from Table 2 in Mitsuiye & Noma, 1992). The value of α_m was 44·3 s^{-1}.

The above results are also different from the recent single channel current analysis in cardiac cells. In Purkinje cells, Scanley *et al.* (1990) obtained very small values of β_i (50±90 and 130±110 s^{-1} at −57 and −52 mV, respectively) based on a five-states Markovian kinetic model. A model of cardiac Na^+ channel with a negligibly small rate constant of inactivation from the open state but significant from the closed state was proposed at potentials of small activation from a convolution analysis of cardiac Na^+ channels by Yue *et al.* (1989: see a scheme in Fig. 3 in their paper). These authors proposed that the inactivation from the open state is steeply voltage dependent (an e-fold change per 28 mV; calculated from 0·9±0·2 equivalent electron charge described). On the contrary, Berman *et al.* (1989), using the approach of Aldrich *et al.* (1983), obtained a rate constant of inactivation from the open state, which was less voltage dependent (an e-fold change per 43 mV) and well comparable to our data (about 400 s^{-1}) at −70 mV in canine ventricular cells. Other earlier studies using the same approach in cardiac cells, however, failed to obtain meaningful results and yielded negative rate constants (Kunze *et al.* 1985; Grant & Starmer, 1987). It might be speculated that the separation of activation kinetics from the inactivation kinetics using a variety of models was not always successful.

Contribution of Na^+ current to the upstroke of action potential

The m^1 activation kinetics, newly determined in the present study, is considered to be pertinent to the physiological action potential, since values of $m(t)$ which were calculated by integrating eqn (7) showed a linear relationship with $P_o(t)N/C_m$ estimated from $dV(t)/dt$ (Fig. 8*B*). It should be noted that the latter parameter is independent of the assumption of the m^1 activation model. In this model fitting, the total number of Na^+ channels was also estimated. The density of the Na^+ channel thus obtained was 1075 pF^{-1}. Assuming 1 $\mu F\ cm^{-2}$, the value gives about eleven channels per μm^2. This value agrees well with ones of ten to fifteen channels per patch in the same preparation, which were determined from the variance–mean relation for the patch current of 5–8 MΩ patch electrodes (Kimitsuki *et al.* 1990). Much smaller values have also been reported in cultured chick myocytes (1–2 per μm^2: Cachelin *et al.* 1983) and neonatal rat ventricular cells (2 per μm^2: Kunze *et al.* 1985). The density of the Na^+ channel is therefore suggested to be high in adult mammalian

cardiac ventricular cells. For this reason, recording single Na^+ channel current may be difficult except in rare cases.

We thank Dr K. Benndorf for his valuable comments on the manuscript. We also thank Mr B. Quinn for correcting the English. This work was supported by Grants-in-Aid for Scientific Research from the Ministry of Education, Science and Culture of Japan.

REFERENCES

ALDRICH, R. W., COREY, D. P. & STEVENS, C. F. (1983). A reinterpretation of mammalian sodium channel gating based on single channel recording. *Nature* **306**, 436–441.

BERMAN, M. F., CAMARDO, J. S., ROBINSON, R. B. & SIEGELBAUM, S. A. (1989). Single sodium channels from canine ventricular myocytes: voltage dependence and relative rates of activation and inactivation. *Journal of Physiology* **415**, 503–531.

BROWN, A. M., LEE, K. S. & POWELL, T. (1981). Voltage clamp and internal perfusion of single rat heart muscle cells. *Journal of Physiology* **318**, 455–477.

CACHELIN, A. B., DE PAYER, J. E., KOKUBUN, S. & REUTER, H. (1983). Sodium channels in cultured cardiac cells. *Journal of Physiology* **340**, 389–402.

COLQUHOUN, D. (1971). *Lectures on Biostatics*. Clarendon Press, Oxford.

GONOI, T. & HILLE, B. (1987). Gating of Na channels: inactivation modifiers discriminate among models. *Journal of General Physiology* **89**, 253–274.

GRANT, A. O. & STARMER, C. F. (1987). Mechanisms of closure of cardiac sodium channels in rabbit ventricular myocytes: single channel analysis. *Circulation Research* **60**, 897–913.

GRANT, A. O., STARMER, C. F. & STRAUSS, H. C. (1983). Unitary sodium channels in isolated cardiac myocytes of rabbit. *Circulation Research* **53**, 823–829.

HAMILL, O. P., MARTY, A., NEHER, E., SAKMANN, B. & SIGWORTH, F. J. (1981). Improved patch-clamp techniques for high resolution current recordings from cells and cell-free membrane patches. *Pflügers Archiv* **391**, 85–100.

HANCK, D. A., SHEETS, M. F. & FOZZARD, H. A. (1990). Gating currents associated with Na^+ channels in canine Purkinje cells. *Journal of General Physiology* **95**, 439–457.

HODGKIN, A. L. & HUXLEY, A. F. (1952). A quantitative description of membrane current and its application to conductance and excitation in nerve. *Journal of Physiology* **117**, 500–544.

HORN, R., VANDENBERG, C. & LANGE, K. (1984). Statistical analysis of single sodium channels: effects of *N*-bromoacetamide. *Biophysical Journal* **45**, 323–336.

HUME, J. R. & UEHARA, A. (1985). Ionic basis of the different action potential configurations of single guinea-pig atrial and ventricular myocytes. *Journal of Physiology* **368**, 525–544.

ISENBERG, G. & KLÖCKNER, U. (1982). Calcium tolerant ventricular myocytes prepared by preincubation in a 'KB medium'. *Pflügers Archiv* **395**, 6–18.

KEYNES, R. D. & ROJAS, E. (1976). The temporal and steady-state relationships between activation of the sodium conductance and movement of the gating particles in the squid giant axon. *Journal of Physiology* **255**, 157–189.

KIMITSUKI, T., MITSUIYE, T. & NOMA, A. (1990). Negative shift of cardiac Na^+ channel kinetics in cell-attached patch recordings. *American Journal of Physiology* **258**, H247–254.

KUNZE, D. J., LACERDA, A. E., WILSON, D. L. & BROWN, A. M. (1985). Cardiac Na^+ current and the inactivating, reopening and waiting properties of single cardiac Na^+ channels. *Journal of General Physiology* **86**, 691–719.

MITSUIYE, T. & NOMA, A. (1987). A new oil-gap method for internal perfusion and voltage clamp of single cardiac cells. *Pflügers Archiv* **410**, 7–14.

MITSUIYE, T. & NOMA, A. (1992). Exponential activation of the cardiac Na^+ current in single guinea-pig ventricular cells. *Journal of Physiology* **453**, 261–277.

OXFORD, G. S. (1981). Some kinetic and steady state properties of Na^+ channels after removal of inactivation. *Journal of General Physiology* **77**, 1–22.

OXFORD, G. S., WU, C. H. & NARAHASHI, T. (1978). Removal of sodium channel inactivation in squid axons by *N*-bromoacetamide. *Journal of General Physiology* **71**, 227–247.

POWELL, T., TERRAR, D. A. & TWIST, V. W. (1980). Electrical properties of individual cells isolated from adult rat myocardium. *Journal of Physiology* **302**, 131–153.

SCANLEY, B. E., HANCK, D. A., CHAY, T. & FOZZARD, H. A. (1990). Kinetic analysis of single sodium channels from canine cardiac Purkinje cells. *Journal of General Physiology* **95**, 411–437.

STIMERS, J. R., BEZANILLA, F. & TAYLOR, R. E. (1985). Sodium channel activation in the squid giant axon: steady-state properties. *Journal of General Physiology* **85**, 65–83.

YUE, D. T., LAWRENCE, J. H. & MARBAN, E. (1989). Two molecular transitions influence cardiac sodium channel gating. *Science* **244**, 349–352.